Synthesis and Characterization of Y-Type Polymers for Second-Order Nonlinear Optical Applications

Balakrishna Kolli,[1] Sarada P. Mishra,[1] Akshaya K. Palai,[1] Tapan Kanai,[1]
M. P. Joshi,[2] S. Raj Mohan,[2] T. S. Dhami,[2] L. M. Kukreja,[2] A. B. Samui[1]
[1]Polymer Science and Technology Centre, Naval Materials Research Laboratory, Shil-Badlapur Road,
Ambernath, Thane 421506, Maharashtra, India
[2]Laser Materials Processing Division, Raja Ramanna Centre for Advanced Technology, Indore 452013,
Madhya Pradesh, India
Correspondence to: A. B. Samui (E-mail: absamui@gmail.com)

Received 30 May 2012; accepted 17 October 2012; published online 8 November 2012
DOI: 10.1002/pola.26439

ABSTRACT: A series of dicyanomethylene-substituted polymers having Y-type molecular architecture were synthesized by Knoevenagel condensation reaction. The polymers were found to be soluble in organic solvents like tetrahydrofuran and chloroform. From gel permeation chromatography, the molecular weights of the polymers were found to be in the range of 15,300–33,800 g/mol. Thermal analysis showed that the polymers were stable up to 350 °C with glass transition temperature (T_g) in the range of 129–212 °C. These polymers were found to form good optical quality films. The order parameter was calculated to be in the range of 0.01–0.48. Atomic force microscopy indicated prominent morphology changes due to alignment of dipoles after poling. By using Nd:YAG laser of 1064 nm, angular dependence and temperature dependence of second-harmonic generation intensity were investigated. The geometry optimization, shape of polymers, and restricted torsion angle between acceptor and donor substituents (push–pull system) were calculated. © 2012 Wiley Periodicals, Inc. J. Polym. Sci., Part A: Polym. Chem. **2013**, *51*, 836–843

KEYWORDS: atomic force microscopy (AFM); corona poling; differential scanning calorimetry (DSC); dipole alignment; glass transition; NLO; order parameter; polymers; relaxation; second-harmonic generation; UV–vis spectroscopy

INTRODUCTION Polymer materials with large nonlinear optical (NLO) responses are of great interest because of their vast applications in optoelectronic technology, such as telecommunications, optical data storage, and optical information processing.[1] Because of their good processability, ultrafast response, chemical flexibility, and large nonlinearity, polymeric materials are more attractive when compared with the traditional inorganic materials like lithium niobate and potassium dihydrogen phosphate.[2] NLO polymers can be synthesized by either doping chromophore into a polymer matrix[3] or by attaching a chromophore covalently to a polymer.[4] In the former process, there is a possibility of decomposition of chromophore at high temperature and immiscibility issue with the host system.[5] Therefore, attaching a chromophore covalently to polymer chain is the preferred way for synthesizing NLO polymer by researchers.

Different types of donors, acceptors, and π-bridges are used to achieve better and long-term properties.[6] The challenging issue is the designing of materials with stable alignment of dipoles after poling. In the quest of stable alignment of dipoles, the most common polymer architecture designed and synthesized was having high glass transition temperature (T_g; e.g., polyimide,[7] polyurethane,[8] and polyester[9]) and also by crosslinking the polymer under poling.[10] In general, the activity of NLO chromophore depends on the donor–acceptor strength and the conjugation length. This aspect has been well studied in various reports.[11] Various substituents on benzene ring have been tried along with oxygen atom as donor. NLO polymers containing other aromatic/nonaromatic system has also been explained in the literature.[12] An heteroaromatic system like phenothiazine is considered to be a highly efficient donor group as it contains both nitrogen and sulfur having lone pair of electrons. The control of function through the primary structure of a molecule is the basis of designing unique architecture such as dendritic architecture.[13]

Taking all these parameters into consideration, Lee and coworkers[14] synthesized various T- and Y-shaped polymers to achieve processable linear polymers similar to that of side-chain systems. Issam has reported that azomethine-based Y-type polyurethane showed reasonable enhancement in thermal stability (T_g) up to 155 °C.[15,16] They observed that the main advantage of this Y shape is that the stability and processability were similar to the main-chain and side-chain polymers, respectively. Two-dimensional Y-type polymers based on 4-(dicyanomethylene)-2-methyl-6-(*p*-(dimethylamino)styryl)-4*H*-pyran (DCM dye) have also been reported.[17,18] Theoretical investigations of DCM derivatives have well encouraged the second-order NLO study.[19] In addition, a large number of donor–acceptor assemblies via self-organization of supramolecular helical dendrimer design and their unique synthesis were reported by Percec et al.[20] Carbazole, naphthalene, and pyrene derivatives have been introduced at the apex as donor groups, and 4,5,7-trinitrofluorene-2-carboxylic acid as donor group glycols were used as spacer. In this way, the charge carrier mobility was found to increase by five orders of magnitude. In another report by the same group, induction of π-stacking of donors at the center of a supramolecular helical pyramidal column was realized by attaching flexible spacer to electron-donor molecules of semifluorinated first-generation self-assembling dendrons.[21] The self-assembling of functional dendrons into supramolecular helical pyramidal columns, containing π-stacks of the electron-acceptor groups having their long axis perpendicular to the axis of the column, was also reported by Percec et al.[22] It was anticipated that the simple and versatile strategy for producing conductive π-stacks of aromatic groups will lead to new classes of supramolecular materials of interest for electronic and optoelectronic applications.

As heteroaromatic moieties have less aromatic stabilization energy that enhances the nonlinearity, phenothiazine-based materials were studied by Choi and coworkers.[23] Polar-ordered thin films were reported for molecules containing phenothiazine.[24] Phenothiazine is an electron-donating group that can facilitate the charge transport of the carrier.[25] Molecular orbital calculation was performed to find out the quantum mechanical parameters. Its strong donor properties were calculated from absorption spectroscopy and electrochemical analysis. The strong donor property of phenothiazine was also confirmed from absorption spectroscopy and theoretical calculation.[26] In the current work, we synthesized different Y-type polymers based on the donor–acceptor–donor–type repeating unit having different aromatic moieties acting as donors and dicyanomethylene acting as an acceptor through conjugated bridge. The donor group is directly linked to the polymer backbone at both the ends, and the acceptor dicyanomethylene group is attached to the pyran ring. The donor is varied from different substituted benzene to phenothiazine.

In the earlier study of Y-type NLO polymer, the chromophore contains nitrogen atom in the donor moiety. Furthermore, in the conventional method, the chromophore was built first, which was then polymerized by attaching with other reactants. However, in this study, the nitrogen in the donor group was replaced by oxygen, and during polymerization, the Y-type structure was developed. The strategy coupled with long alkane chain in the polymer is expected to give better solubility characteristics. After confirming the structures of the polymers, their other properties such as thermal stability, T_g, surface morphology, and their second-harmonic generation (SHG) activity were investigated.

EXPERIMENTAL

Materials

4-Hydroxybenzaldehyde (98%; Fluka, Switzerland), vanillin (99%; S.D. Fine Chemicals, India), phenothiazine (98%; Lancaster, England), and 2,6-dimethyl-4*H*-pyran-4-one, syringaldehyde, and malononitrile were purchased from Sigma-Aldrich, Germany, and used as received. Piperidine and pyridine were dried by standard procedure. Compounds 2-(2,6-dimethyl-4*H*-pyran-4-ylidene)malononitrile (**1**)[18(e)] and 4,4′-[hexane-1,6-diylbis(oxy)]bis(3-methoxybenzaldehyde) (**3**)[27] were synthesized as per the literature procedure.

Characterization Techniques

Fourier transform infrared (FTIR) spectra were recorded on Perkin-Elmer 1600 series FTIR spectrophotometer using KBr pellets. UV–visible spectra were taken on a Varian (Cary 500) scan UV–Vis–NIR spectrophotometer. ^{1}H NMR spectra were recorded either on 400 MHz or 500 MHz Bruker spectrometer using $CDCl_3$ as solvent, and ^{13}C NMR spectra were recorded on 300 MHz Jeol spectrometer. Chemical shifts were determined by using tetramethylsilane as an internal standard. Molecular weight distributions were determined by using gel permeation chromatography on Waters 2690 separations module using a Waters 2410 refractive index detector with tetrahydrofuran (THF) as an eluent (flow rate = 1 mL/min) and polystyrene as calibration standards. Thermogravimetric analyzer (TGA; TA Instruments His Res TGA 2950) was used for thermal analysis, with a heating rate of 20 °C/min in N_2 atmosphere. The thermal transitions were determined by using differential scanning calorimeter (TA Instruments) with heating rate of 10 °C/min in N_2 atmosphere. Thickness of the film was measured by using Alpha-step surface profiler. Melting point of the monomers was recorded by an electrothermal 9100 melting point apparatus.

Thin Film Preparation

For making thin film of the polymers, indium tin oxide (ITO) glass substrates were precleaned thoroughly with dimethylformamide (DMF), distilled water, methanol, and acetone in ultrasonic bath. About 3 wt % chloroform solution of polymer was filtered through 0.25-μ PTFE filter, and then the solution was spin coated on an ITO glass slide at a rotation speed of 1200 rpm for 60 s at room temperature. Finally, the cast films were dried in vacuum for 12 h at room temperature to remove the trace amount of the solvent. The film thicknesses were found to be in the range of 0.54–1.13 μm.

Corona Poling and SHG Measurement

The polymer-coated ITO glass was mounted on a heating stage. The distance of the film was maintained to be 1 cm from the tip of the tungsten needle. An electric field of 4.8 kV was applied through the needle at a temperature slightly higher than the T_g of polymer. The poled polymer film was characterized by using UV–vis spectroscopy. The order parameter (Φ) was calculated by using the following equation:[28]

$$\Phi = 1 - A_1/A_0,$$

where A_0 and A_1 are the absorbance of the polymer film before and after poling, respectively.

The second-order NLO effect of poled films was found out by SHG experiment. For measuring the SHG intensity, 1064-nm-pulsed Nd:YAG laser of pulse width 5 ns and 10 Hz repetition rate, with laser energy of 5 mJ, was used. In this process, poled films were mounted on rotational stage for checking angular dependence of the SHG intensity. The fundamental beam from the generated SHG signal was blocked by IR filter. The SHG signal was detected by a photomultiplier tube, and the signal was averaged by using an oscilloscope.

Synthesis of Monomers and Polymers

Synthesis of 4,4′-[Hexane-1,6-diylbis(oxy)] dibenzaldehyde (2)

4-Hydroxybenzaldehyde (2.0 g, 0.016 mmol) and potassium carbonate (6.0 g, 0.049 mmol) were taken in a 100-mL round-bottomed flask containing 25 mL of DMF and stirred for 15 min at room temperature. 1,6-Dibromohexane (2.0 g, 8.19 mmol) was then charged into it and stirred for 24 h by maintaining the temperature at 90 °C. The reaction mixture was precipitated in excess water, and the product was extracted thrice with chloroform. The crude compound was recrystallized from ethanol and chloroform (9:1 v/v) mixture.

Yield: 85%; mp: 110 °C; FTIR (KBr): ν (cm^{-1}) 2947, 2846, 2753, 1686, 1598, 1254, 1158. ^{1}H NMR (CDCl$_3$, 400 MHz): δ (ppm) 9.8 (s, 2H), 7.84 (d, J = 8.0 Hz, 4H), 7.0 (d, J = 8.0 Hz, 4H), 4.08 (t, J = 8.0 Hz, 4H), 1.88 (m, 4H), 1.59 (m, 4H). ^{13}C NMR (CDCl$_3$, 75 MHz): δ (ppm) 190, 165, 131.9, 131.5, 114, 68, 28, 25.

Synthesis of 4,4′-[Hexane-1,6-diylbis(oxy)] bis(3,5-dimethoxybenzaldehyde) (4)

A similar procedure was followed to synthesize Compound **2**.

Yield: 85%; mp: 80 °C; FTIR (KBr): ν (cm^{-1}) 3011, 2972, 2854, 2746, 1682, 1581, 1236, 1038. ^{1}H NMR (CDCl$_3$, 400 MHz): δ (ppm) 9.86 (s, 2H), 7.26 (s, 4H), 4.10 (t, J = 8.0 Hz, 4H), 3.91 (s, 12H), 1.81 (m, 4H), 1.55 (m, 4H). ^{13}C NMR (CDCl$_3$, 75 MHz): δ (ppm) 191, 153, 143, 131, 106, 73, 56, 30, 25.

Synthesis of 1,6-Di(10H-phenothiazin-10-yl)hexane (5)

Phenothiazine (2.0 g, 0.01 mol) and sodium hydroxide (2.4 g, 0.06 mol) were taken in a round-bottomed flask containing 25 mL of DMSO, and then the mixture was stirred for 20 min. 1,6-Dibromohexane (1.22 g, 5.02 mmol) was then added slowly, and the temperature was maintained at 70 °C for 6 h. The reaction mixture was cooled to room temperature and added into water. The compound was extracted with chloroform, washed with water, dried in MgSO$_4$, and evaporated. The crude material was purified by column chromatography.

Yield: 47%; mp: 152 °C; FTIR (KBr): ν (cm^{-1}) 3060, 2926, 2850, 2583, 1596, 1333, 1247, 752. ^{1}H NMR (CDCl$_3$, 400 MHz): δ (ppm) 7.14 (m, 8H), 6.91 (m, 8H); 3.82 (t, J = 12.0 Hz, 4H), 1.79 (m, 4H), 1.46 (m, 4H). ^{13}C NMR (CDCl$_3$, 75 MHz): δ (ppm) 145, 127.4, 127.1, 124, 122, 115, 47, 26.6, 26.4.

Synthesis of 10,10′-(Hexane-1,6-diyl)bis(10H-phenothiazine-3-carbaldehyde) (6)

Compound **5** (0.7 g, 1.45 mmol) was taken in a round-bottomed flask containing 15 mL of dichloroethane and 1 mL of DMF. The solution was cooled in an ice bath, and then 0.7 mL of POCl$_3$ was added slowly. The ice bath was removed; the reaction mixture was refluxed for 9 h and poured into an aqueous sodium acetate solution. The compound was extracted with chloroform, washed with water, dried, and evaporated. The crude product was purified by column chromatography.

Yield: 52%; mp: 140 °C; FTIR (KBr): ν (cm^{-1}) 3055, 2931, 2855, 2721, 1687, 1592, 1366, 1166, 748. ^{1}H NMR (CDCl$_3$, 400 MHz): δ (ppm) 9.79 (s, 2H), 7.63–7.56 [m (br), 4H], 7.17–6.83 (m, 10H), 3.88 (t, J = 4.0 Hz, 4H), 1.8 (m, 4H), 1.47 (m, 4H). ^{13}C NMR (CDCl$_3$, 75 MHz): 189.9, 150, 143, 131, 129, 128, 127.6, 127.5, 125, 124, 123, 116, 114, 47, 26.5, 26.2.

Representative Example of Polymerization

2-(2,6-Dimethyl-4*H*-pyran-4-ylidene)malononitrile (**1**; 0.1 g, 0.58 mmol) and Compound **2** (0.18 gm, 0.58 mmol) were charged in a 25-mL round-bottomed flask connected to a Schlenk tube. To the solution, 3 mL of dry pyridine and 0.1 mL of piperidine (1.16 mmol) were charged and refluxed for 60 h. The polymer was precipitated in excess methanol, and the solid was separated by filtration. It was purified by soxhlation with methanol to remove oligomers. The polymer was dried under vacuum for 24 h at room temperature.

Polymer P1. Yield: 85%; FTIR (KBr, cm^{-1}): 3033, 2936, 2860, 2199, 1604, 1580, 1427, 1249. ^{1}H NMR (CDCl$_3$, 500 MHz): δ (ppm) 7.54–7.40 (m, 4H), 7.0–6.86 (m, 4H), 6.84–6.78 (m, 2H), 6.76–6.69 (m, 2H), 4.08–3.80 (m, 4H), 1.9–1.4 (m, 8H).

Polymer P2. Yield: 89%; FTIR (KBr, cm^{-1}): 2997, 2936, 2855, 2199, 1644, 1583, 1422, 1266. ^{1}H NMR (CDCl$_3$, 500 MHz): δ (ppm) 7.45–7.35 (m, 2H), 7.03–6.89 (m, 4H), 6.84–6.58 (m, 6H), 4.13–3.68 (m, 10H), 2.10–1.4 (m, 8H).

Polymer P3. Yield: 70%; FTIR (KBr, cm^{-1}): 2999, 2932, 2855, 2199, 1694, 1583, 1417, 1227. ^{1}H NMR (CDCl$_3$, 500 MHz): δ (ppm) 7.13–7.08 (m, 4H), 6.66–6.61 (m, 4H), 6.45–6.38 (m, 2H), 4.09–3.69 (m, 16H), 1.90–1.38 (m, 8H).

Polymer P4. Yield: 94%; FTIR (KBr, cm^{-1}): 3060, 2936, 2844, 2204, 1638, 1533, 1466, 1255. ^{1}H NMR (CDCl$_3$, 500 MHz): δ (ppm) 7.7–7.0 (m, 14H), 6.9–6.5 (m, 6H), 3.90–3.49 (m, 4H), 1.9–1.1 (m, 8H).

RESULTS AND DISCUSSION

Synthesis and Characterization

Synthetic routes for monomers and polymers are shown in Schemes 1 and 2, respectively. First, 2-(2,6-dimethyl-4*H*-pyran-4-ylidene)malononitrile (**1**) was obtained by reacting

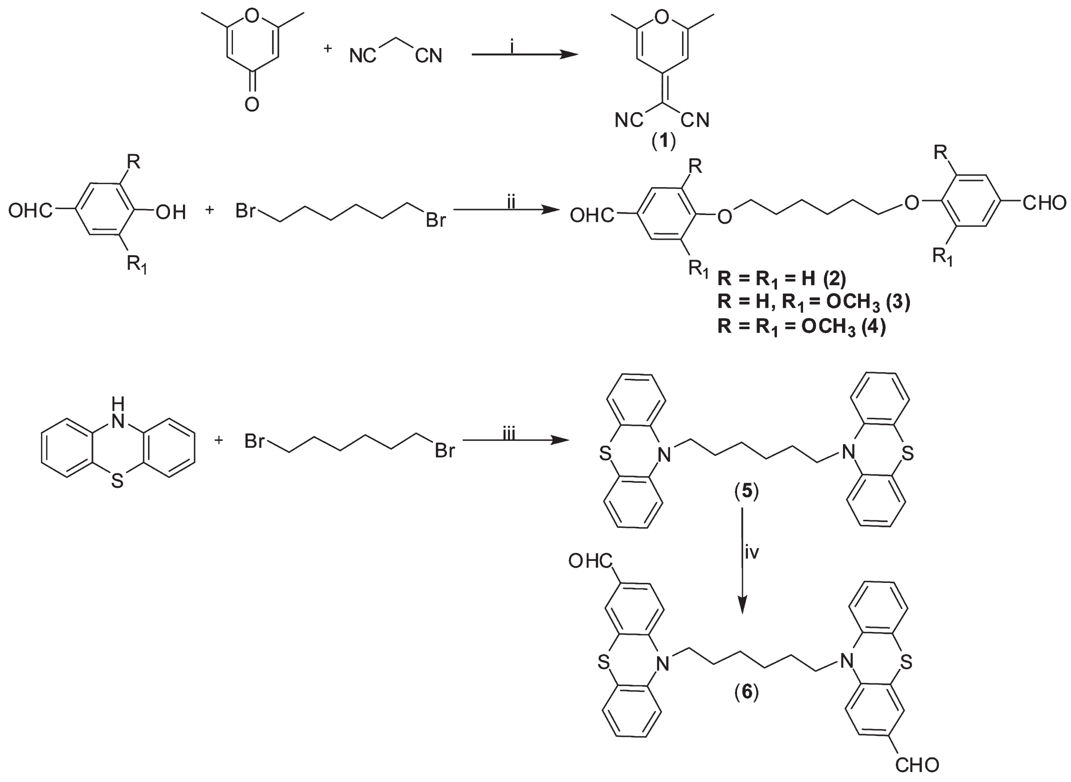

SCHEME 1 Synthesis of monomers.

2,6-dimethyl-4*H*-pyran-4-one with malononitrile. *p*-Hydroxybenzaldehyde, vanillin, syringaldehyde, and phenothiazine were treated with 1,6-dibromohexane in the presence of base to afford Compounds **2**–**5**. Compound **5** was further subjected to standard Vilsmeier–Haack reaction to get aldehyde **6** in good yield.[29] All the monomers showed characteristic peaks in ^{1}H NMR and particularly the peak around 9.7–9.8 ppm, confirming the presence of aldehyde proton. FTIR spectra of monomers showed characteristic peaks near 1680 cm^{-1} for carbonyl stretching. Figure 1 shows a strong peak near 2200 cm^{-1}, which is characteristic of cyano group. All the monomers (**2**–**4** and **6**) were then reacted with equivalent moles of Compound **1** in pyridine and a catalytic amount of piperidine to afford the polymers **P1**–**P4** with

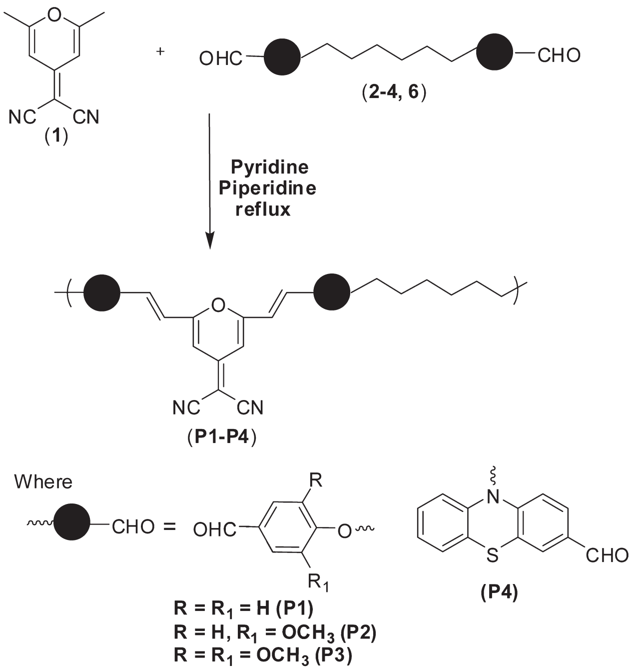

SCHEME 2 Synthesis of Y-type polymers.

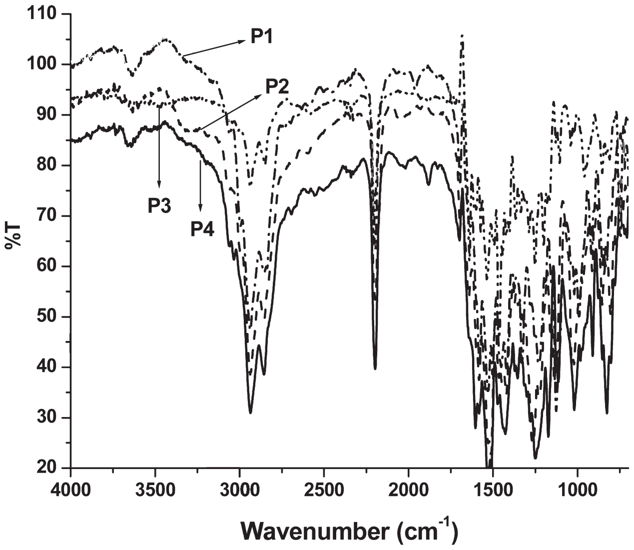

FIGURE 1 IR spectra of polymers.

TABLE 1 Polymer Characterization Data

Polymer	λ_{max} (nm)^a	M_w^{b}	PDI^b	T_g (°C)^c	Φ^d
P1	417	33,800	2.4	172	0.30
P2	340	19,600	1.7	129	0.20
P3	337	18,200	1.7	133	0.07
P4	459	15,300	1.5	212	0.48

[a] Wavelength at which maximum absorption was observed.
[b] Calculated from gel permeation chromatography.
[c] Glass transition temperature of polymers found from differential scanning calorimetry.
[d] Order parameter measured from UV–vis spectra.

good yield. In ^{1}H NMR, appearance of a peak at 6.9–6.6 ppm confirmed the presence of stilbene double bond. A small peak for aldehyde proton was also observed, indicating that the polymers formed were not of very high molecular weight.

The polymers were soluble in organic solvents like THF and chloroform with molecular weights in the range of 15,300–33,800 g/mol and polydispersity index 1.5–2.4 (Table 1). The TGA thermogram showed weight loss of 10% around a temperature range of 366–374 °C (Fig. 2). The higher thermal stability may be due to the two-dimensional structures of the chromophores in the polymer, which has been well explained by Hsiue and coworkers.[30] The T_g of the polymers (**P1**–**P2**) were in the range of 129–212 °C. A drop in the T_g of polymers **P2** and **P3** from that of **P1** may be due to the combined effect of lower molecular weight and the presence of methoxy group substitutions on the benzene ring. The polymer **P4** showed enormous enhancement in T_g despite its lowest molecular weight, which may be due to the condensed nitrogen-containing aromatic ring[31] and two-dimensional structure of the polymer.

Figure 3 shows the electronic spectra of the thin film of polymer **P1**. The absorption data of the polymers in thin film are shown in Table 1. It can be observed that the donor structure has influenced the absorption pattern of the polymer as the acceptor remained same. The wavelength of maximum absorbance (λ_{max}) depends on the conjugation length and the donor strength.

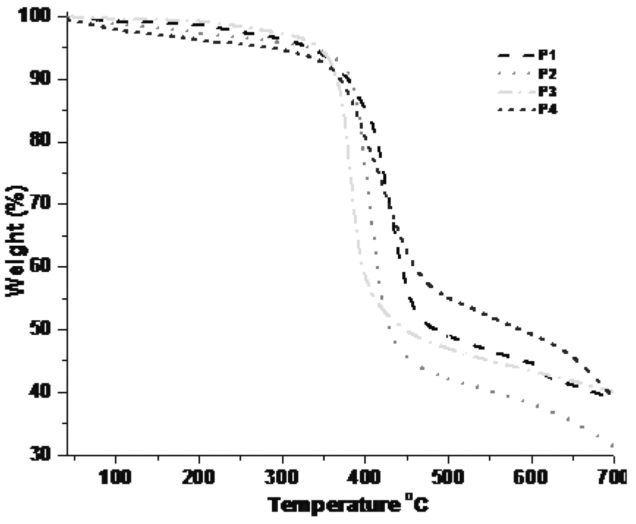

FIGURE 2 TGA thermogram of polymers **P1**–**P4**.

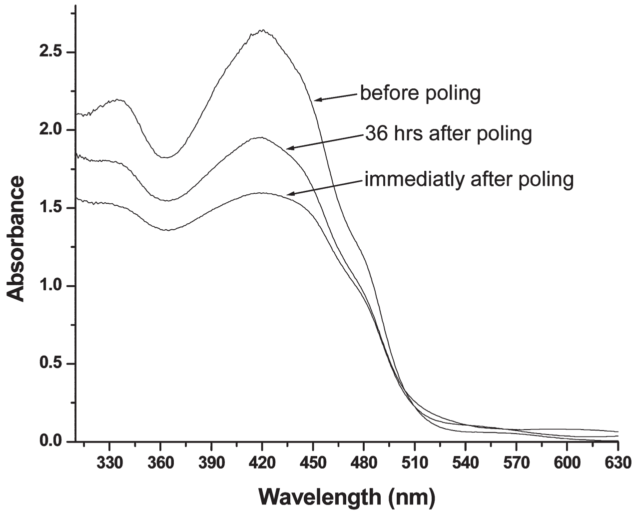

FIGURE 3 UV–vis absorption spectra of polymer **P1**.

Corona Poling and Optical Properties

Optically transparent thin films of the polymers (**P1**–**P4**) were cast from chloroform solution over ITO glass slides for measuring their SHG intensity. Initially, the thin films of polymers are in centrosymmetric fashion due to the dipole–dipole interaction. After applying the electric field (4.8 kV), the temperature was gradually increased to 10 °C above the T_g. The polymer film was then maintained for 30 min under the applied voltage. Finally, the film was cooled to room temperature in the presence of electric field to freeze the aligned dipoles in noncentrosymmetric fashion, which was confirmed by the electronic spectra. The representative electronic spectra (Fig. 3) showed decrease in absorption after poling due to birefringence.[32] From change in absorption pattern, the order parameter (Φ) was calculated and found to be 0.07–0.48, which is better than the azo polymer in our earlier report[33] (Table 1). Figure 4 shows surface morphology of the polymer **P3** obtained by atomic force microscopy. Figure 4(b) shows the development of well-defined hills and valleys after poling. This change in original micrograph indicates alignment of dipoles, which is well known in the literature.[34]

The second-order NLO properties were studied by SHG method. By using Nd:YAG laser of IR wavelength (1064 nm), the angular dependence was studied. Figure 5 shows the angular dependence of SHG intensity of polymer **P1**. It can be observed that the SHG intensity increases with the angle of incidence and reaches a maximum at around 50°. Then it decreases with further increase in the angle of incidence. This is due to maximum interaction of laser with dipole at a particular angle.

By increasing the temperature of the poled film, the dynamic thermal stability of poled dipoles was also studied. For this, the temperature of the poled film was increased at the rate

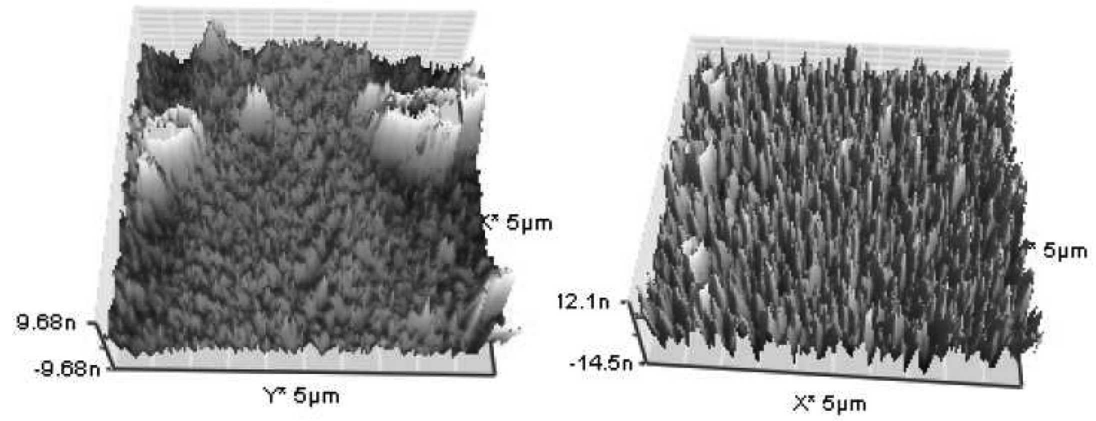

(a) (b)

FIGURE 4 Atomic force microscopy of **P3** before (a) and after (b) poling.

of 4 °C/min (from room temperature). Figure 6 shows the dynamic thermal stability of polymers **P1**, **P2**, and **P4**. It can be seen that SHG intensity of **P2** is stable up to 100 °C, whereas **P1** is stable up to 110 °C. This could be due to the higher T_g value of **P1** when compared with **P2** (also **P3**, which relaxed very fast and attained less SHG intensity). This results in higher segmental mobility of P2 making the dipoles relax easily. However, when the system changes to heteroaromatic moiety containing polymer **P4**, the SHG intensity remains stable up to almost 165 °C.

Theoretical Calculations

To examine the effect of monomethoxy- and dimethoxy-substituted benzene and phenothiazine in the geometry of designed polymers on the torsion angle, energies, and so forth, computational study was executed. Although correlation between experimental and theoretical data differs slightly for various methods, they are useful for trend predictions in the molecular design of new compounds for NLO applications.

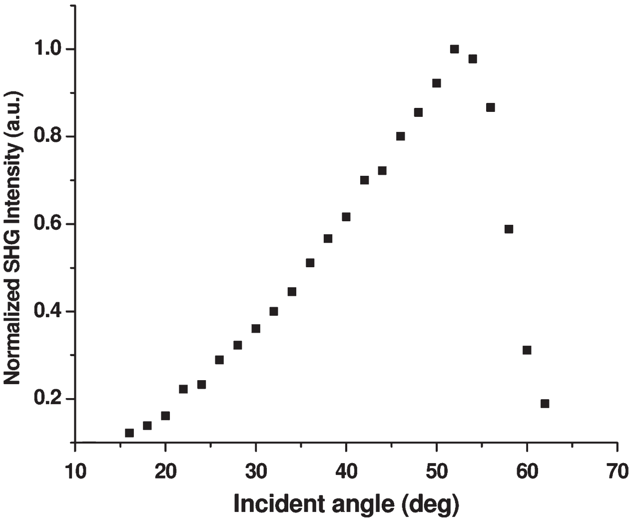

FIGURE 5 SHG intensity of poled film **P1** as a function of incident angle.

Forcite calculates single-point energy and performs geometry optimization, that is, energy minimization of polymers and periodic systems.[35] The study focuses on atomistic simulations of polymer; the main interest being the performance of classical models. The polymer-consistent force field developed for synthetic polymers forms the basis for the simulations. The simulated structures of the polymers are shown in Figure 7.

The shapes of polymers **P1**–**P3** are found to be zigzag in nature where repeating unit is Y-type. The acceptor (pull unit) groups and donor (push unit) groups are found orthogonal (opposite regiomers) to each other. The orientation of these groups has large contribution to the net dipole moment and consequently on SHG intensity of polymer. In case of **P4**, although Y shape is maintained, the shape of the polymer is similar to a ribbon.

The calculated energy of the polymers strongly depends on the conformational statistics of the polymer chains and the force field. The total energy can be given as follows:[36]

$$V = \sum_{\text{valence energy}} V_{\text{diag. terms}} + \sum_{\text{valence energy}} V_{\text{cross terms}} + \sum_{\text{nonbonded energy}} V$$

The total energies for all the four types of dimers are summarized in Table 2. The energy values are found to be at maximum in case of **P3**. It is important to note that polymer **P3** having methoxy substituents on benzene ring has large steric effect, which might be responsible for high energy value. The polymer **P1** has the lowest energy value, indicating its maximum stability. However, **P4** has the energy slightly higher than **P1**, indicating high stability as well as high electron-donating ability. This imparts higher order parameter and stability of SHG signal over longer period. The restricted torsion angle determined for all polymers are summarized in Table 3. The torsion angle of donor unit and

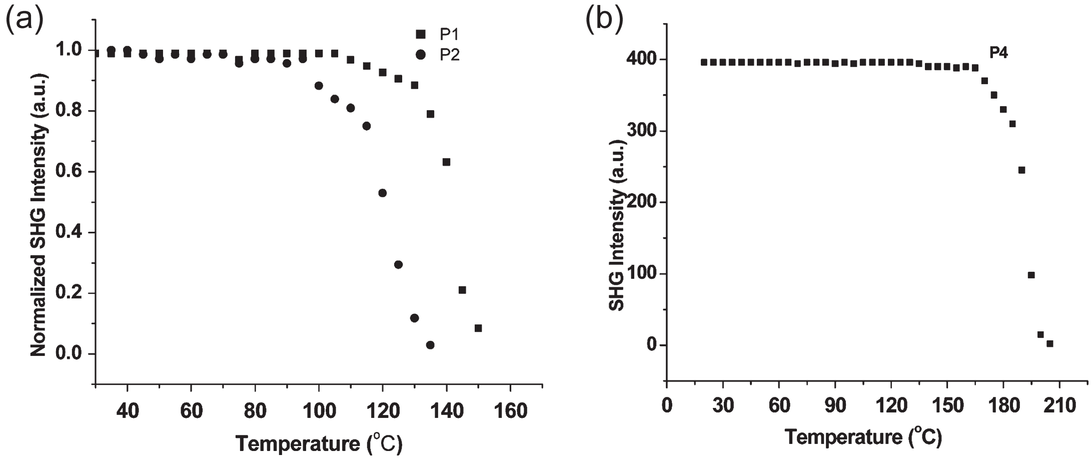

FIGURE 6 SHG intensity of poled polymers **P1** and **P2** (a) and **P4** (b) as a function of temperature.

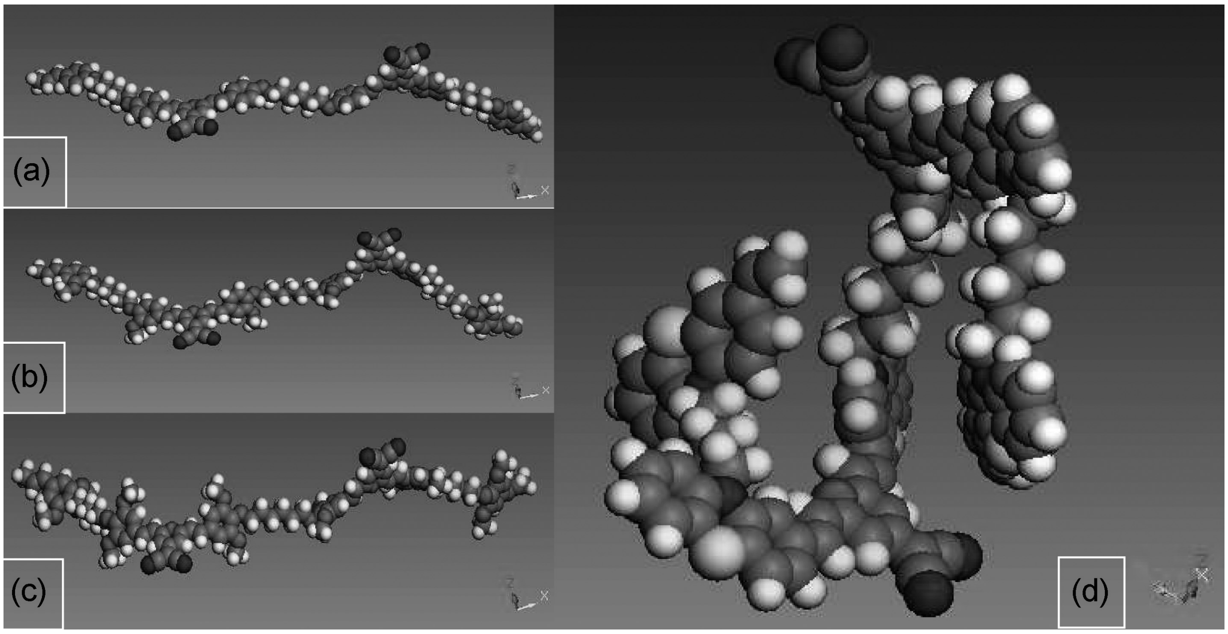

FIGURE 7 Simulation results in material studio (polymer-consistent force field, atom based): (a) **P1**; (b) **P2**; (c) **P3**; and (d) **P4**.

acceptor unit do not deviate much from coplanarity, indicating sufficient high second-order nonlinearity.

CONCLUSIONS

Four Y-type polymers were successfully synthesized by Knoevenagel condensation. The polymers were thermally stable up to 350 °C. The glass transition temperatures of all polymers were above 129 °C and ranging up to 212 °C. These polymers easily formed good optical quality films from their chloroform solution. The solid films remained stable at high electric field (4.8 kV) during poling. Electronic spectra showed decrease in absorption due to poling, and particularly for polymer **P4**, the order parameter was quite high at 0.48. In addition, polymer **P4** also exhibited higher SHG intensity and high thermal stability.

TABLE 2 Calculated Energies of Dimers from Modeling Study

Polymer	Total Energy (kcal/mol)
P1	81.568
P2	166.806
P3	229.702
P4	149.509

TABLE 3 Restricted Torsion Angle of Polymers

Torsion Angle	P1	P2	P3	P4
C2-C1-C13-C15	1.64	3.09	5.18	2.2
C4-C5-C12-C14	7.59	4.21	2.42	11.53
C3-C7-C8-N9	1.86	132.92	26.06	19.14
C3-C7-C10-N11	5.83	25.66	33.20	43.97

REFERENCES AND NOTES

1 (a) P. N. Prasad, D. J. Williams, Introduction to Nonlinear Optical Effects in Molecules and Polymers; Wiley: New York, **1991;1** (b) G. A. Lindsay, K. D. Singer, Polymers for Second-Order Nonlinear Optics; American Chemical Society: Washington, DC, **1995.**

2 D. M. Burlabd, R. D. Miller, C. A. Walsh, *Chem. Rev.* **1994,** *94*, 31–75.

3 (a) G. R. Meredith, J. VanDusen, D. J. Williams, *Macromolecules* **1982,** *15*, 1385–1389; (b) F. Li, K.-H. Kim, J. J. Kulig, E. P. Savitski, W. J. Brittain, F. W. Harris, S. Z. D. Cheng, S. F. Hubbard, K. D. Singer, *J. Mater. Chem.* **1995,** *5*, 253–259.

4 (a) N. Nemoto, F. Miyata, Y. Nagase, J. Abe, M. Hasegawa, Y. Shirai, *Macromolecules* **1996,** *29*, 2365–2371.

5 (a) K. D. Singer, M. G. Kuzyk, J. E. Sohn, *J. Opt. Am. B* **1987,** *4*, 968–976; (b) M. A. Firestone, M. A. Ratner, T. J. Marks, *Macromolecules* **1995,** *28*, 6296–6310.

6 (a) E. Gubbelmans, T. Verbiest, M. V. Beylen, A. Persoons, C. Samyn, *Polymer* **2002,** *43*, 1581–1585; (b) L. Yu, W. K. Chan, Z. Peng, A. Gharavi, *Acc. Chem. Res.* **1996,** *29*, 13–21.

7 (a) D. Yu, A. Gharavi, L. Yu, *Macromolecules* **1996,** *29*, 6139–6142; (b) M. H. Kim, J. Jin, C. J. Lee, N. Kim, K. H. Park, *Bull. Korean Chem. Soc.* **2002,** *23*, 964–970; (c) D. Yu, A. Gharavi, L. Yu, *J. Am. Chem. Soc.* **1995,** *117*, 11680–11686; (d) T.-A. Chen, A. K.-Y. Jen, Y. Cai, *J. Am. Chem. Soc.* **1995,** *117*, 7295–7296.

8 J.-Y. Lee, W.-J. Lee, E.-J. Park, H.-B. Bang, B. K. Rhee, C. Jung, S. M. Lee, J. H. Lee, *Bull. Korean Chem. Soc.* **2003,** *24*, 1727–1728.

9 (a) J.-Y. Lee, J. H. Kim, W. T. Jung, *Bull. Korean Chem. Soc.* **2007,** *28*, 329–332; (b) J.-Y. Lee, W.-T. Jung, W.-J. Lee, *Polym. Int.* **2006,** *55*, 248–256.

10 (a) K. S. Han, S. K. Park, S. Y. Shim, W. S. Jahng, N. J. Kim, *Bull. Korean Chem. Soc.* **1998,** *19*, 1165–1168; (b) A. Scarpaci, E. Blart, V. Montembault, L. Fontaine, V. Rodriguez, F. Odobel, *Chem. Commun.* **2009,** *14*, 1825–1827.

11 K. S. David, A. Hemeryck, N. Tancrez, L. Toupet, J. A. G. Williams, I. Ledoux, J. Zyss, A. Boucekkine, J.-P. Guegan, H. L. Bozec, O. Maury, *J. Am. Chem. Soc.* **2006,** *128*, 12243–12255.

12 (a) Z. Li, Z. Qin, S. Li, C. Ye, *Synth. Met.* **2003,** *135*, 467–468; (b) D. W. Kim, S. Hong, S. Y. Park, N. Kim, *Bull. Korean Chem. Soc.* **1997,** *18*, 198–203.

13 J. G. Rudick, V. Percec, *Acc. Chem. Res.* **2008,** *41*, 1641–1652.

14 (a) H.-N. Jang, J.-Y. Lee, *Bull. Korean Chem. Soc.* **2008,** *29*, 933–938; (b) D.-S. Won, G.-Y. Lee, J.-Y. Lee, *Dyes Pigments* **2008,** *78*, 225–230; (c) J.-Y. Lee, H.-B. Bang, E.-J. Park, W.-J. Lee, B. K. Ree, S. M. Lee, *Polym. Int.* **2004,** *53*, 1838–1844; (d) H. J. No, H.-N. Jang, Y. J. Cho, J. Y. Lee, *J. Polym. Sci. Part A: Polym. Chem.* **2010,** *48*, 1166–1172.

15 A. M. Issam, *Eur. Polym. J.* **2007,** *43*, 214–219.

16 J.-Y. Lee, H.-B. Bang, E.-J. Park, C. S. Baek, B. K. Rhee, S. M. Lee, *Synth. Met.* **2004,** *144*, 159–167.

17 F. G. Webster, W. C. McColgin, U.S. Patent 3,852,683, **1974.**

18 (a) C. R. Moylan, S. Ermer, S. M. Lovejoy, I.-H. McComb, D. S. Leung, R. Wortmann, P. Krdmer, R. J. Twieg, *J. Am. Chem. Soc.* **1996,** *118*, 12950–12955; (b) B. Villacampa, R. Andreu, E. Galan, J. Garin, V. Herrero, E. Lacarra, J. Orduna, R. Alicante, *J. Org. Chem.* **2010,** *75*, 1684–1692; (c) E. Gubbelmans, K. V. Broeck, T. Verbiest, M. Beylen, A. Persoons, C. Samyn, *Eur. Polym. J.* **2003,** *39*, 969–976; (d) S. Ermer, S. M. Lovejoy, D. S. Leung, H. Warren, C. R. Moylan, R. J. Twieg, *Chem. Mater.* **1997,** *9*, 1437–1442; (e) A. Carella, F. Borbone, U. Caruso, R. Centore, A. Roviello, A. Barsella, A. Quatela, *Macromol. Chem. Phys.* **2007,** *208*, 1900–1907.

19 Y. Liu, Y. Liu, H. Hu, C. Liu, *J. Mol. Struct.* **2001,** *570*, 43–51.

20 V. Percec, M. Glodde, T. K. Bera, Y. Miura, J. Shiyanovskaya, K. D. Singer, V. S. K. Balagurusamy, P. A. Heiney, I. Schnell, A. Rapp, H.-W. Spiess, S. D. Hudson, H. Duan, *Nature* **2002,** *419*, 384–387.

21 V. Percec, M. Glodde, M. Peterca, A. Rapp, I. Schnell, H. W. Spiess, T. K. Bera, Y. Miura, V. S. K. Balagurusamy, E. Aqad, P. A. Heiney, *Chem.—Eur. J.* **2006,** *12*, 6298–6314.

22 V. Percec, E. Aqad, M. Peterca, M. R. Imam, M. Glodde, T. K. Bera, Y. Miura, V. S. K. Balagurusamy, P. C. Ewbank, F. Wurthner, P. A. Heiney, *Chem.—Eur. J.* **2007,** *13*, 3330–3345.

23 (a) M. J. Cho, S. K. Lee, J. Jin, D. H. Choi, L. R. Dalton, *Thin Solid Films* **2006,** *515*, 2303–2309; (b) S. K. Lee, M. J. Cho, H. Yoon, S. H. Lee, J. H. Kim, Q. Zhang, D. H. Choi, *Macromol. Res.* **2004,** *12*, 484–489.

24 W. Hung, M. Helvenston, J. L. Casson, R. Wang, J.-F. Bardeau, Y. Lee, M. S. Johal, B. I. Swanson, J. M. Robinson, D. Li, *Langmuir* **1999,** *15*, 6510–6514.

25 M. J. Cho, J. Y. Kim, J. H. Kim, S. H. Lee, L. R. Dalton, D. H. Choi, *Bull. Korean Chem. Soc.* **2005,** *26*, 77–84.

26 S. K. Lee, M. J. Cho, G. W. Kim, W. G. Jun, J. Jin, L. R. Dalton, D. H. Choi, *Opt. Mater.* **2007,** *29*, 451–456.

27 A. K. Palai, S. K. Rath, R. Srivastava, M. N. Kamalasanan, M. Patri, *J. Appl. Polym. Sci.* **2009,** *112*, 2988–2998.

28 Q. Pan, C. Fang, Z. Qin, Q. Gu, X. Cheng, D. Xu, J. Yu, *Mater. Lett.* **2003,** *57*, 2612–2615.

29 J. Simokaitiene, A. Danilevicius, S. Grigalevicius, J. V. Grazulevicius, V. Getautis, V. Jankauskas, *Synth. Met.* **2006,** *156*, 926–931.

30 P.-H. Chang, J.-Y. Chen, H.-C. Tsai, G.-H. Hsiue, *J. Polym. Sci. Part B: Polym. Chem.* **2009,** *47*, 4937–4949.

31 S. P. Mishra, A. K. Palai, A. Kumar, R. Srivastava, M. N. Kamalasanan, M. Patri, *Macromol. Chem. Phys.* **2010,** *211*, 1890–1899.

32 J. Y. Lee, H. B. Bang, E. J. Park, B. K. Rhee, S. M. Lee, J. H. Lee, *J. Polym. Sci Part A: Polym. Chem.* **2004,** *42*, 3189–3199.

33 A. S. Rekha, D. Ratna, A. B. Samui, *J. Appl. Polym. Sci.* **2007,** *103*, 4425–4431.

34 (a) H. J. No, H.-N. Jang, Y. H. Cho, J.-Y. Lee, *J. Polym. Sci. Part A: Polym. Chem.* **2010,** *48*, 1166–1172; (b) S.-H. Lee, Y.-S. Kang, S.-J. Song, *Chem. Commun.* **1998,** *22*, 2513–2514.

35 V. Srinivasa Rao, A. B. Samui, *J. Polym. Sci. Part A: Polym. Chem.* **2009,** *47*, 2774–2786.

36 S. Pandey, S. P. Mishra, B. Kolli, T. Kanai, A. B. Samui, *J. Polym. Sci. Part A: Polym. Chem.* **2012,** *50*, 2659–2668.